UCRL-JC-121629
PREPRINT

Development of XUV-Interferometry (155Å) Using a Soft X-ray Laser

L. B. Da Silva, T. W. Barbee, R. Cauble,
P. Celliers, D. Ciarlo, S. Libby, R. A. London,
D. L. Matthews, S. Mrowka, J. C. Moreno,
J. E. Trebes, A. S. Wan, and F. Weber

This paper was prepared for submittal to the
SPIE 40th Annual Meeting
San Diego, CA
July 9-14, 1995

August 1, 1995

Lawrence Livermore National Laboratory

Development of xuv-interferometry (155 Å) using a soft x-ray laser

L.B. Da Silva, T.W. Barbee, Jr., R. Cauble, P. Celliers, D. Ciarlo, S. Libby, R.A. London, D.L. Matthews, S. Mrowka, J.C. Moreno, J.E. Trebes, A.S. Wan and F. Weber

Lawrence Livermore National Laboratory
P.O. Box 808, M/S L-447,Livermore CA, 94550

ABSTRACT

Over the past several years we have developed a variety of techniques for probing plasmas with x-ray lasers. These have included direct high resolution plasma imaging to quantify laser produced plasma uniformities and moiré deflectometry to measure electron density profiles in one-dimension. Although these techniques have been valuable a need existed for direct two dimensional measurements of electron densities in large high density plasmas. For this reason we have worked on developing a xuv interferometer compatible with the harsh environment of laser produced plasmas. This paper describes our design and presents some results showing excellent fringe visibility using the neon-like yttrium x-ray laser operating at 155Å. The coherence properties of this x-ray laser source were measured using interferometry and are also discussed.

Keywords: x-ray lasers, interferometry, plasma diagnostics, multilayer optics, coherence measurements

1. INTRODUCTION

The high brightness and comparatively routine operation of existing collisionally pumped soft x-ray lasers has opened up the possibility of using these systems for a variety of applications. The use of Ni-like tantalum x-ray laser for biological imaging has already been demonstrated[1] and will ultimately allow us to study biological specimens in a natural environment with resolutions far exceeding that possible with optical techniques. The high brightness of saturated x-ray lasers[2,3,4,5] also makes them an ideal tool for probing high density and large plasmas relevant to astrophysics and inertial confinement fusion (ICF).

The Ne-like yttrium x-ray laser is well suited to this application by virtue of its high output energy (~8 mJ)[5] and monochromatic output (i.e. dominated by 155Å, J=2-1). The wavelength is also well suited to existing multilayer mirror technology which have demonstrated reflectivities of ~60%. At LLNL we have now used this system to image accelerated foils[6] and measure electron density profiles[7] in a laser irradiated target using moiré deflectometry. More recently we have performed experiments to demonstrate x-ray laser interferometry. In contrast to other techniques interferometry offers the possibility of directly measuring the electron density profile in large and high density plasmas.

In the study of laser produced plasmas optical interferometry has played a key role in the accurate measurements of electron density profiles for a variety of target conditions. Profile steepening due to radiation pressure was first quantified by Attwood et al.[8] using a short pulse 2650 Å optical interferometer. It has been used to measure electron density profiles in exploding foils under conditions relevant to x-ray lasers[9,10]. The filamentation instability in laser produced plasmas was investigated by Young et al.[11,12] also using optical interferometry. In all these cases, however, the size of the plasma and the peak electron density accessible were severely restricted by absorption and refraction. In laser produced plasmas, inverse bremsstrahlung absorption becomes significant for optical probes at electron densities exceeding 10^{20} cm^{-3}. Refraction of the probe beam is sensitive to electron density gradients and ultimately affects spatial resolution and data interpretation[13]. These problems are particularly significant as we push forward to producing and studying large (3 mm) and high density plasmas (10^{22} cm^{-3}) relevant to inertial confinement fusion (ICF)[14] and astrophysics[15]. For these reasons there has existed a need to develop interferometry techniques at soft x-ray wavelengths where absorption and refraction effects can be mitigated.

Extending conventional interferometric techniques into the soft x-ray range has been difficult because of the problems with designing optical systems which operate in the range 40-400Å. Reflective/grating systems have been discussed in the literature and have been used successfully at 1246Å[16]. A purely reflective Fresnel bimirror setup has been demonstrated by Svatos et al.[17] at 48Å. Both of these technique, however, lack some of the advantages of standard interferometer geometries. Fortunately, multilayer mirror technology has now evolved to the point where artificial structures can be routinely fabricated with reflectivities as high as 65% at 130Å [18,19] and with the overall uniformities required by more conventional interferometers.

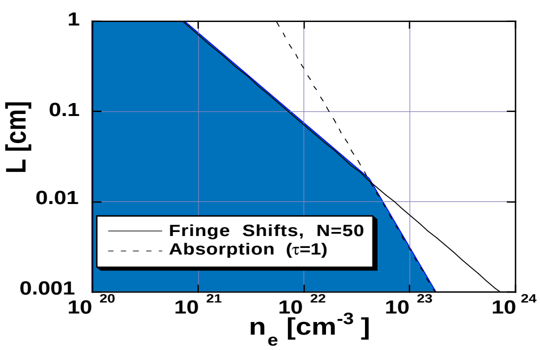

Figure 1 Shaded area is accessible parameter space of electron density and plasma size (L) constrained by absorption (assuming only free-free, T_e=1 keV, <Z>=30, λ=155 Å)

In a plasma with electron density n_e, the index of refraction, n_{ref} is related to the critical electron density, $n_{cr} = 1.1\times10^{21}\lambda^{-2}$ [cm^{-3}] (λ in μm), by $n_{ref} = \sqrt{1-\frac{n_e}{n_{cr}}}$. In an interferometer the number of fringe shifts, N_{Fringe}, is then given by

$$N_{Fringe} = \frac{\delta\phi}{2\pi} = \frac{1}{\lambda}\int_0^L (1-n_{ref})\,dl \approx \frac{n_e}{2n_{cr}}\frac{L}{\lambda}$$

where the integral is along ray trajectories through the plasma, dl, is the differential path length, L is the plasma length and we assume refraction effects are negligible. Experimentally the maximum number of fringe shifts measurable is usually constrained by detector resolution and is rarely greater than ~50. This imposes a constraint on the product n_eL for a given wavelength. An additional constraint which limits the accessible density and length parameter space is absorption. In a plasma dominated by free-free absorption the absorption coefficient, α, is approximately given by[20]

$$\alpha \approx 2.44\times10^{-37}\frac{\langle Z^2\rangle n_e n_i}{\sqrt{kT}\,(h\nu)^3}\left[1-\exp\left(\tfrac{-h\nu}{kT}\right)\right] \qquad \mathrm{cm}^{-1} \qquad (1)$$

where the electron temperature, kT, and photon energy, $h\nu$, are in eV and electron and ion density are in cm^{-3}. The strong scaling with photon energy shows the advantage of probing with soft x-ray sources. For most high temperature plasmas of interest, the level of ionization is sufficient to eliminate any bound-free absorption in the soft x-ray region. Resonant line absorption is possible but very unlikely given the narrow bandwidth of the x-ray laser ~10 mÅ[21]. Therefore, if we consider only free-free absorption in a plasma with 1 keV temperature and average ionization 30 (mid-Z plasma) we obtain from Eq. 1, $\alpha \approx 2.6\mathrm{x}10^{-43} n_e^2$ for λ=155Å. If we allow for one optical depth (i.e. $\alpha L = 1$) of absorption we obtain $n_e^2 L = 3.8\mathbf{x}10^{42}$. In Figure 1 we show the electron density and plasma dimension accessible with a soft x-ray laser source (155 Å) which is constrained by free-free absorption and a maximum of 50 fringe shifts. At the higher densities the accessible parameter space is limited by absorpiton but it easily covers all plasmas normally produced in the laboratory.

The adverse effects of refraction[10] can be significantly reduced by using a short wavelength probe. In Figure 2 we compare the deflection angle after propagating through a 3mm plasma for an optical (2650Å) and xuv (155Å) probe source. At a fundamental level large deflection angles imply significant spatial blurring and reduced spatial resolution. In addition, since probe rays will propagate through a range of electron densities interpretation of the results will be more difficult. Another important advantage of using xuv probes is that spatial resolutions of better than 1µm can be easily achieved by using normal incidence spherical multilayer mirrors.

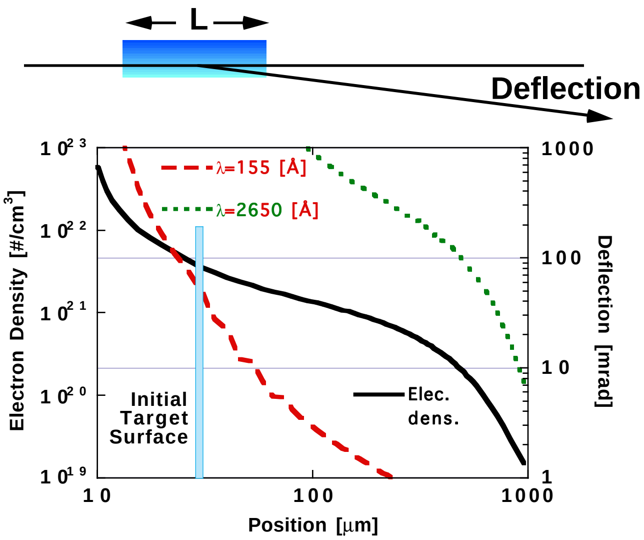

Figure 2 Calculated electron density (t=0.9 ns after start of pulse) for a CH target irradiated at 2.0×10^{13} W/cm^2 and the deflection assuming a 3 mm wide plasma (L) for probe laser wavelength of 2650 Å and 155 Å.

Although direct imaging with x-ray lasers has its advantages it does not require several of the attributes of the x-ray laser, specifically small source size, narrow divergence and narrow bandwidth. The drawback of direct imaging for plasma studies is that in order to determine the electron density of these plasmas it is necessary to have an accurate estimate of the opacity. For high-Z systems this can be a near impossible problem at soft x-ray wavelengths. For this reason we have pushed towards the development of moiré deflectometry (which measures electron density gradients) and interferometry which is a direct measurement of electron density. For a detailed discussion of our progress in moiré deflectometry see the paper by Ress et al.[7]. In this paper we describe the development of an XUV interferometer and its use in characterizing the coherence characteristics of the yttrium x-ray laser.

2. DESIGN OF XUV INTERFEROMETER

The development of xuv interferometry has only recently become possible because of the progress made in the fabrication of high quality beam splitters. The beam splitters we utilize have a 1 cm square opening and consist of 1000Å of silicon nitride with 8 layer pairs of Mo/Si. These splitters have a reflectivity of 25±5% and transmission of 20±5%. The experimental setup we have used to demonstrate xuv interferometry is shown in Figure 3. The x-ray laser beam is collected with a spherical multilayer mirror (50cm focal length) which collimates the beam and injects the beam into a Mach-Zehnder interferometer. Multilayer mirror damage issues constrained the design of the interferometer to have segment lengths of 50cm (i.e. total length of each arm is 100cm). In addition, given the temporal coherence length of ~50µm for our x-ray laser it was necessary to prealign this interferometer using a white light source. The second plasma is imaged with a spherical mirror onto a backside illuminated CCD detector. The multilayer mirrors consist of 15 layer pairs of Mo/Si and have a measured reflectivity of 60±5% at normal incidence. In our imaging experiments we have used a variety of imaging mirrors ranging in focal length from 11cm to 50cm (f# 20) and magnifications of 3 to 30. Multilayer mirror damage due to side scattered laser light is a serious problem for mirror to plasma distances less than 25cm and high optical laser energies (1-2kJ) on the secondary target. The effective bandpass of the multilayer mirror and filter combination is 8Å centered at 155Å. Ideally the bandpass would be comparable to the x-ray laser spectral width of ~7x10^{-3}Å in order to further reduce background emission. The spatial resolution of this imaging system has been measured to be better than 1µm and is limited by the CCD detector pixel size of 24µm and spherical aberrations and astigmatism due to off-axis operation.

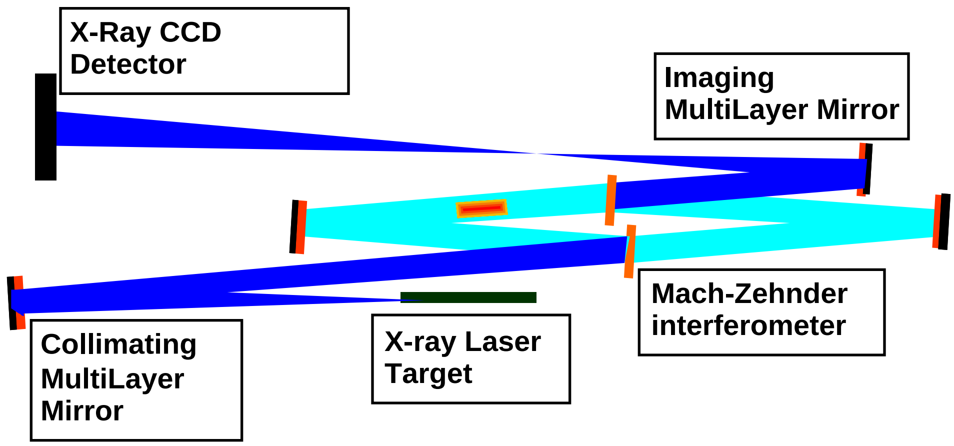

Figure 3. Experimental setup used for xuv interferometry

In Figure 4a we show an interferogram obtained using this system without a secondary plasma. The results show excellent fringe visibility and prove the viability of this technology. In Figure 4b we show a low fringe visibility interferogram obtained when low tension beam splitters were used. These splitters were extremely sensitive to vibrations and the low fringe visibility of these splitters may be due to splitter motion during the x-ray laser pulse. At these wavelengths motions of 20 Å within the 200ps pulse width correspond to velocities of 10 m/sec which could be possible. By adjusting the manufacturing technique we have, however, been able to produce beam splitters reliably that avoid this problem. The interferometer developed in this project is now routinely used to measure electron density profiles in a variety of laser produced plasmas (refer to article by A.S. Wan et al. in these proceedings).

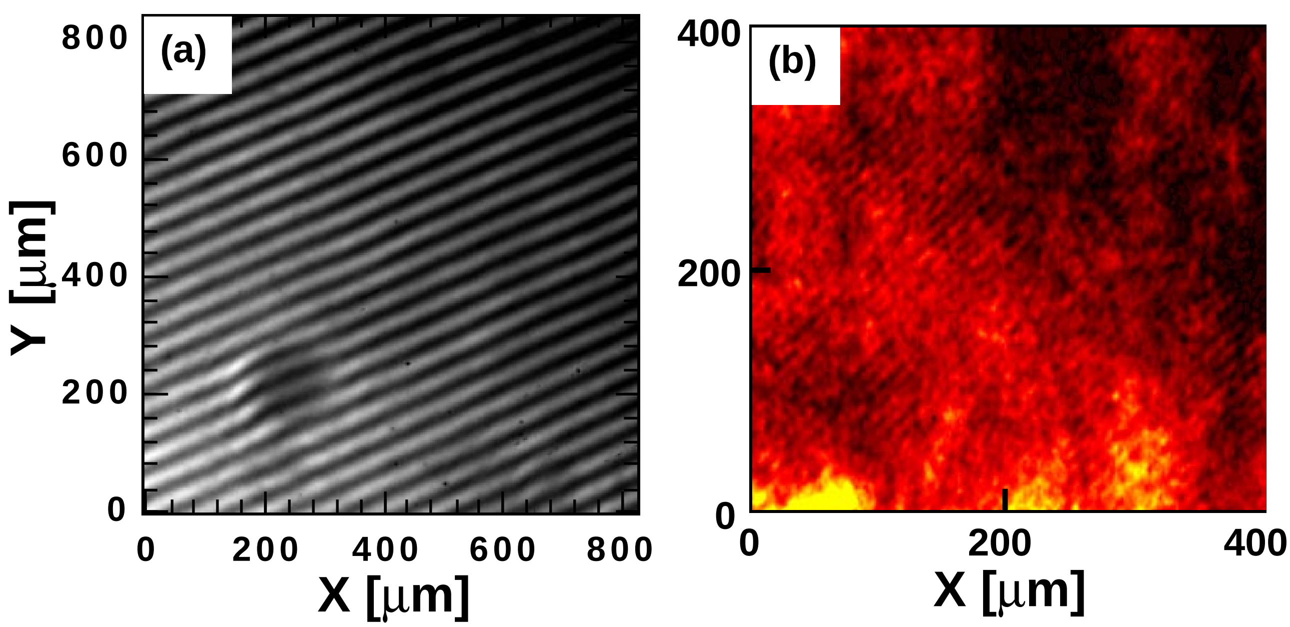

Figure 4. Interferograms obtained using neon-like yttrium x-ray laser λ=155 Å, a) using high stress silicon nitride membranes and b) low stress.

3. COHERENCE MEASUREMENTS OF X-RAY LASER USING INTERFEROMETRY

A unique application of interferometry is to accurately measure the coherence properties of the source. Using a second Mach-Zehnder interferometer we have performed experiments to quantify the longitudinal and transverse coherence of the yttrium x-ray laser. In Figure 5 we show the experimental setup used for this measurement. The output from the x-ray laser is propagated into a secondary chamber where an identical interferometer is positioned. The distance from the x-ray laser source to the first beam splitter is 200cm. A filter consisting of 1000Å of Lexan and 2000Å aluminum was placed at the entrance of the chamber to eliminate stray optical light. An additional filter consisting of 2000Å of Lexan and 2000Å of titanium was placed in front of the CCD to attenuate the signal. The total filter attenuation was 5×10^{-5}. In order to measure the longitudinal coherence multilayer mirror M1 was translated to vary the path length difference of the two interferometer arms. Figure 6a shows the fringe pattern observed over the full 1cm by 1cm aperture of the beam splitters. The total figure error is approximately 30 fringes. This measurement is consistent with optical interferograms obtained of the individual beam splitters. We are currently planning to obtain optically polished thick silicon substrates which should yield a better figure.

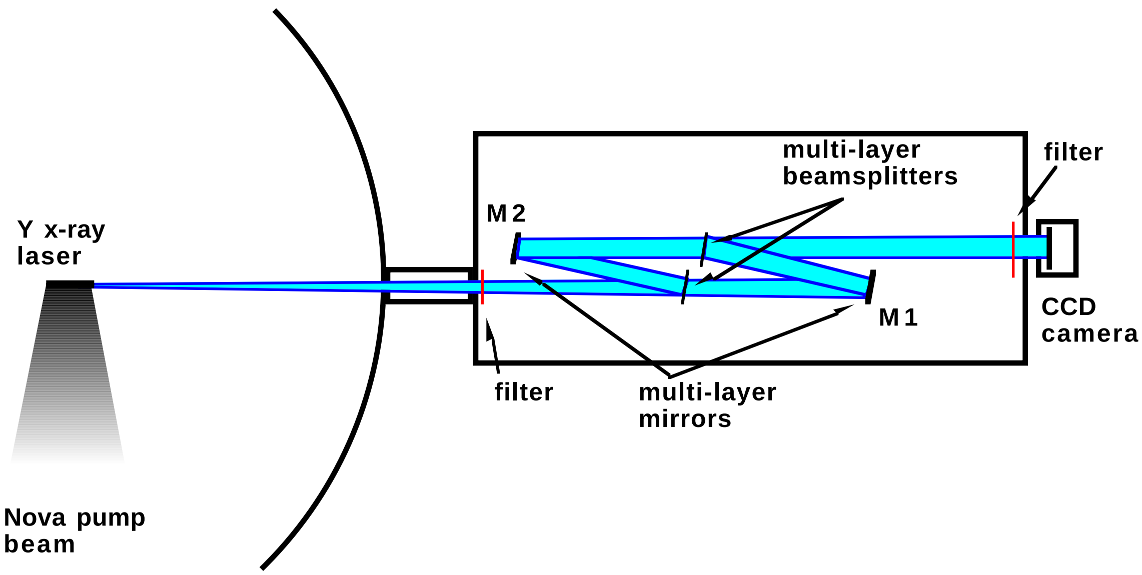

Figure 5. Experimental setup used to measure the coherence properties of the yttrium x-ray laser. .

In figure 6 we show the interferograms obtained when the optical path difference was 0, 50, 125 and 250 µm. A clear reduction in fringe visibility occurs as the path difference increases. In figure 7 we plot the measured fringe visibility, defined as $V = (I_{\max} - I_{\min})/(I_{\max} + I_{\min})$, as a function of optical path difference. The fringe visibility we measure is equal to the magnitude of the complex degree of coherence of the illumination beam[22]; this latter quantity is directly related to the power spectral density, $G(\nu)$, of the beam through a Fourier transform relation (Wiener-Khinchin theorem)[23]. Assuming a gaussian line shape for the Y laser, $G(\nu) \propto \exp\left[-\left(2\sqrt{\ln 2}\left(\nu - \bar{\nu}\right)/\Delta\nu\right)^2\right]$, where $\bar{\nu} = c/\lambda$ and ν is the FWHM linewidth (c is the speed of light). The fringe visibility is the envelope of the autocorrelation function for this power spectrum, which varies with path difference, c, according to $V(\tau) = \exp\left[-\left(\pi\,\Delta\nu\,\tau/\left(2\sqrt{\ln 2}\right)\right)^2\right]$. A gaussian fit to the measured fringe visibility yields a $1/e$ half-width of c=100 µm yielding in turn an equivalent gaussian FWHM linewidth of 13mÅ for the x-ray laser line. This value is similar to 11mÅ reported for the collisionally pumped Se x-ray laser operating at 20.6 nm, in which significant gain narrowing was observed when the laser became saturated[21]. For an expected ion temperature of 600 eV the intrinsic Doppler broadened linewidth of the Y laser transition[24] is expected to be around 31mÅ, thus the determination of 13mÅ inferred from this measurement also indicates that the laser line undergoes gain narrowing.

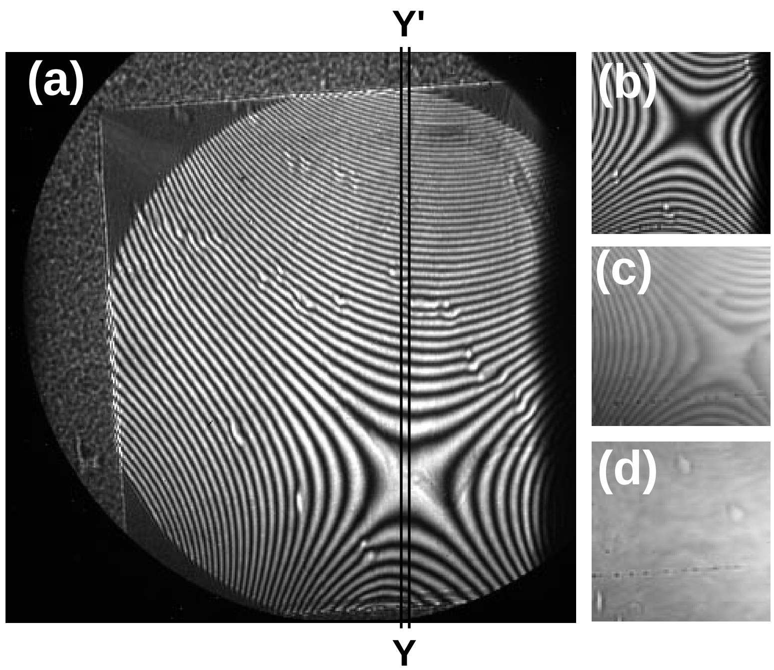

Figure 6. Interferograms obtained at different optical path differences a) 0 μm, b) 50 μm, c) 125 μm, and d) 250 μm.

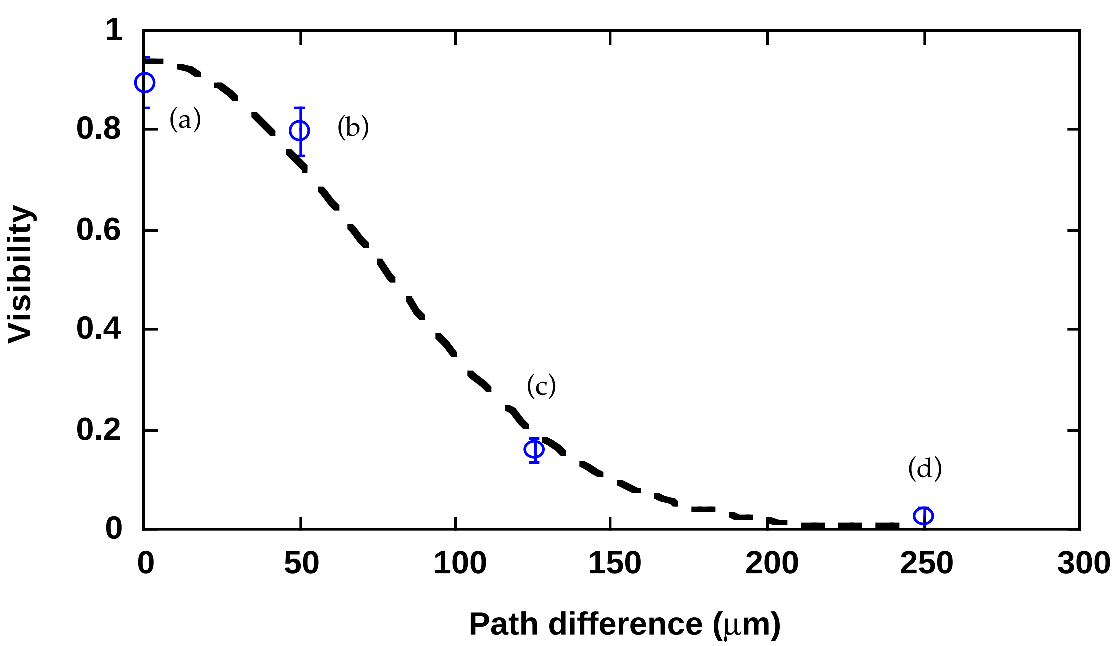

Figure 7. Measured fringe visibility in interferograms of figure 6 and the best fit gaussian.

In regions away from the null point of the saddle distribution the fringe visibility diminishes. We can exploit this situation to obtain a rough characterization of the spatial coherence of the illumination beam. The aberration in the beam splitters which produces the saddle pattern distorts the local propagation direction of the recombined beams relative to one another in a manner that varies over the field. The fringe frequency, k, gives a measure of the local relative angle, θ, of the recombined beams, through the relation, $k = 2\pi \sin\theta / \lambda$. After propagation through a sufficiently large distance various parts in the aberrated regions of the recombined beams become spatially separated by a distance proportional to the local relative angle. This spatial separation is given by the relation $\Delta x \approx L \sin\theta = kL\lambda / 2\pi$, where L is the distance from the detector plane to the surface where the distortion is introduced. Figure 8 displays a plot of the variation of fringe visibility with fringe frequency along the line Y-Y' displayed in Figure 6.

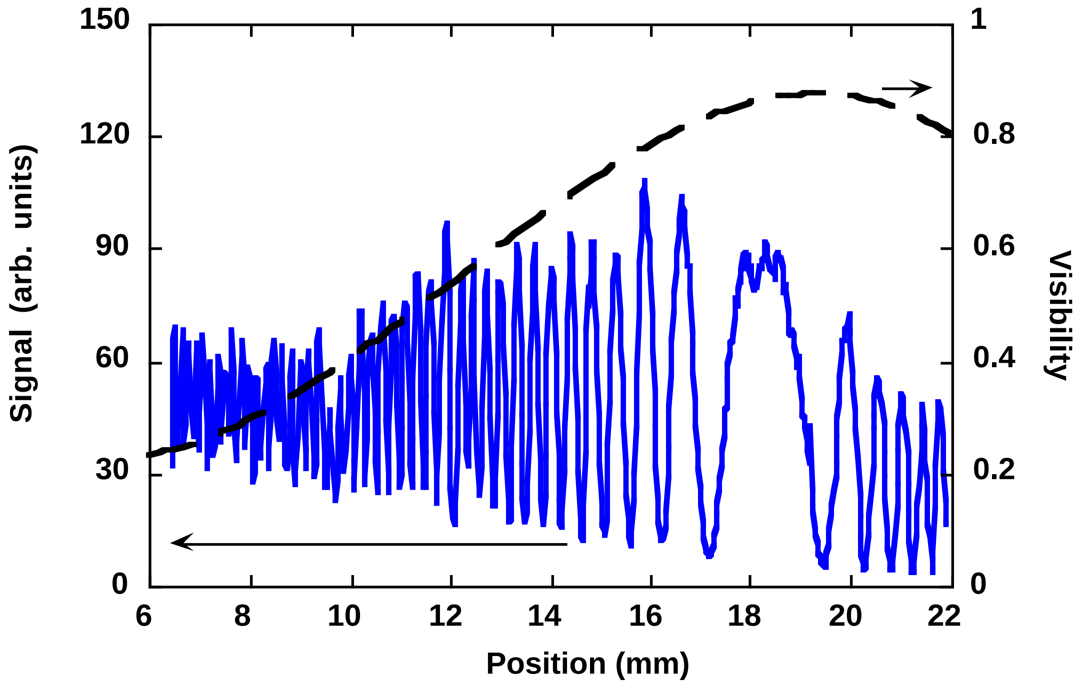

Figure 8. Intensity plot along line Y-Y' in figure 6a (solid line) clearly showing the change in fringe visibility (dashed line) as a function of fringe spacing. .

In the aberrated regions of the recombined beam the fringe visibility measures the magnitude of the complex coherence factor of the source, *i.e.* $V = |\mu(\Delta x, \Delta y)|$ where μ is the complex coherence factor; x and y represent the differences of coordinates in the recombined beams. An equation, derived from the Van Cittert-Zernicke theorem, relates the complex coherence factor to the coherence area, A_C, of the beam[23], $A_c \equiv \iint_{-\infty}^{\infty} |\mu(\Delta x, \Delta y)|^2 d\Delta x d\Delta y$. We can fit the measured fringe visibility to a gaussian function $V(\Delta x) \approx \exp\left[-(\Delta x / a)^2\right]$, with a=0.16 mm. Assuming an azimuthally symmetric spatial coherence distribution for the beam (*i.e.* $\Delta x = \Delta r$, where r is the radial coordinate) we can evaluate this integral for A_C yielding $A_C \approx 0.040$ mm2. One can now relate the coherence area measured at a large distance, d, to the source area, A_S, through the equation[23] $A_c = (\lambda d)^2 / A_s$. Applying this relation to our measured parameters we find an effective source diameter of ≈ 220 μm FWHM at the output of the x-ray laser. This determination of the source area of the x-ray laser illumination beam is about 1.8 times larger than the size of the observed emission region from the x-ray laser inferred from previous measurements[25,26], but within the estimated ±50% uncertainty bounds as discussed above.

3. CONCLUSIONS

The high brightness of x-ray lasers make them ideally suited for studying long scalelength and high density plasmas. Using a yttrium x-ray laser and a multilayer coated Mach-Zehnder interferometer we have demonstrated the potential advantages of xuv probing to diagnose high density plasmas relevant to ICF and astrophysics. Using this interferometer we have demonstrated its use to measure the coherence properties of x-ray lasers with a compact diagnostic. Future developments should allow us to adapt this technology to demonstrate Fourier transform spectroscopy in the xuv with potentially high spectral resolution.

4. ACKNOWLEDGMENTS

The authors are indebted to Joe Kilkenny and the Nova Experiments Group for their support and assistance in these experiments. We would also like to thank Sharon Alvarez, Jim Cox and Ken Haney for their contributions. This work was supported by USDOE/OHER, and performed under the auspices of the U.S. Department of Energy by the Lawrence Livermore National Laboratory under Contract No. W-7405-ENG-48.

5. REFERENCES

1. L. B. Da Silva, J. E. Trebes, R. Balhorn, S. Mrowka, E. Anderson, D. T. Attwood, T. W. Barbee, J. Brase, M. Corzett, J. Gray, J. A. Koch, C. Lee, D. Kern, R. A. London, B. J. MacGowan, D. L. Matthews and G. Stone, *X-ray Laser Microscopy of Rat Sperm Nuclei* , Science 258, 269-271(1992)

2. A. Carillon, H. Z. Chen, P. Dhez, L. Dwivedi, J. Jacoby, P. Jaegle, G. Jamelot, J. Zhang, M. H. Key, A. Kidd, A. Klisnick, R. Kodama, J. Krishnan, C. L. S. Lewis, D. Neely, P. Norreys, D. O'Neill, G. J. Pert, S. A. Ramsden, J. P. Raucourt, G. J. Tallents and J. Uhomoibhi, *Saturated and Near-Diffraction-Limited Operation of an XUV Laser at 23.6 nm* , Phys. Rev. Lett. 68, 2917-2920(1992)

3. S. Wang, Y. Gu, G. Zhou, Y. Ni, S. Yu, S. Fu, C. Mao, Z. Tao, W. Chen, Z. Lin, D. Fan, G. Zhang, J. Sheng, M. Yang, T. Zhang, Y. Shao, H. Peng and X. He, *Experimental Research on Saturated Gain for soft x-ray Laser from Neon-like Germanium Plasma* , Chinese Phys. Lett. 8, 618(1991)

4. B. J. MacGowan, L. B. Da Silva, D. J. Fields, C. J. Keane, J. A. Koch, R. A. London, D. L. Matthews, S. Maxon, S. Mrowka, A. L. Osterheld, J. H. Scofield, G. Shimkaveg, J. E. Trebes and R. S. Walling, *Short Wavelength X-ray Laser Research at the Lawrence Livermore National Laboratory* , Phys. Fluids 4, 2326-2337(1992)

5. L. B. Da Silva, B. J. MacGowan, S. Mrowka, J. A. Koch, R. A. London, D. L. Matthews and J. H. Underwood, *Power measurements of a saturated yttrium X-ray laser* , Optics Lett. 18, 1174-1176(1993)

6. R. Cauble, L. B. Da Silva, J. T.W. Barbee, P. Celliers, J. C. Moreno and A. S. Wan, *Micron-resolution radiography of laser-accelerated and x-ray heated foils with an x-ray laser* , Phys. Rev. Lett. 74, 3816-3819(1995)

7. D. Ress, L. B. Da Silva, R. A. London, J. E. Trebes, S. Mrowka, R. J. Procassini, J. T.W. Barbee and D. E. Lehr, *Measurement of Laser-Plasma Electron Density with a Soft X-ray Laser Deflectometer* , Science 265, 514-517(1994)

8. D. T. Attwood, D. W. Sweeney, J. M. Auerbach and P. H. Y. Lee, *Interferometric Confirmation of Radiation-Pressure Effects in Laser-Plasma Interactions* , Phys. Rev. Lett. 40, 184-186(1978)

9. G. Charatis, G. E. Busch, C. L. Shepard, P. M. Campbell and M. D. Rosen, *Hydrodynamic aspects of selenium x-ray laser targets* , Journal De Physique C6, 89-98(1986)

10. M. K. Prasad, K. G. Estabrook, J. A. Harte, R. S. Craxton, R. A. Bosch, G. E. Busch and J. S. Kollin, *Holographic Interferograms from laser fusion code simulations* , Phys. Fluids B 4, 1569-1575(1992)

11. P. E. Young, *Experimental study of filamentation in laser-plasma interactions* , Phys. Fluids B 3, 2331-2336(1991)

12. S. Wilks, P. E. Young, J. Hammer, M. Tabak and W. L. Kruer, *Spreading of Intense Laser Beams Due to Filamentation* , Phys. Rev. Lett. 73, 2994-2997(1994)

13. L. B. Da Silva, B. Cauble, G. Freiders, J. A. Koch, B. J. MacGowan, D. L. Matthews, S. Mrowka, D. B. Ress, J. E. Trebes and T. L. Weiland, *Imaging with x-ray lasers* , Proc. SPIE 2012, 158(1994)

14. B. G. Levi, *Veil of secrecy is lifted from parts of livermore's laser fusion program* , Physics Today September, 17-19(1994). M.D. Cable et al., Phys. Rev. Lett. 73, 2316(1994). L.J. Suter et al., Phys. Rev. Lett. 73, 2328(1994). T.R. Dittrich et al., Phys. Rev. Lett. 73, 2324(1994). R.L. Kauffman et al., Phys. Rev. Lett. 73, 2320(1994).

15. T. S. Perry, S. J. Davidson, F. J. D. Serduke, D. R. Bach, C. C. Smith, J. M. Foster, R. J. Doyas, R. A. Ward, C. A. Iglesias, F. J. Rogers, J. J. Abdallah, R. E. Stewart, J. D. Kilkenny, and R. W. Lee, *Opacity Measurements in a Hot Dense Medium*, Phys. Rev. Lett. 67, 3784 (1991). L. B. Da Silva, B. J. MacGowan, D. R. Kania, B. A. Hammel, C. A. Back, E. Hsieh, R. Doyas, C. A. Iglesias, F. J. Rogers and R. W. Lee, *Absorption Measurements demonstrating the importance of $\Delta n=0$ Transitions in the Opacity of Iron* , Phys. Rev. Lett. 69, 438-441(1992)

16. S. Chakrabarti, D. M. Cotton, J. S. Vickers and B. C. Bush, *Self-compensating, all reflection interferometer* , Appl. Opt. 33, 2596-2602(1994)

17. J. Svatos, D. Joyeux, D. Phalippou and F. Polack, *Soft-x-ray interferometer for measuring the refractive index of materials* , Optics lett. 18, 1367-1369(1993)

18. T. W. Barbee Jr., J. C. Rife, W. R. Hunter, M. P. Kowalski, R. G. Cruddace and J. F. Seely, *Long-term stability of a Mo/Si multilayer structure* , Appl. Opt. 32, 4852-4854(1993)

19. D. G. Stearns, R. S. Rosen and S. P. Vernon, *Fabrication of high reflectance Mo/Si multilayer mirrors by planar magnetron sputtering* , J. Vac. Sci. Technol. A, Vac. Surf. Films 9, 2662-2669(1991)

20. C. W. Allen, *Astrophysical Quantities* (Oxford University Press, New York, 1963).

21. J. Koch, B. J. MacGowan, L. B. D. Silva, D. L. Matthews, J. H. Underwood, P. J. Batson and S. Mrowka, *Observation of gain-narrowing and saturation behavior in Se x-ray laser line profiles* , Phys. Rev. Lett. 68, 3291(1992)

22. M. Born and E. Wolf, *Principles of Optics* (Pergamon Press, Oxford, 1980).

23. J. W. Goodman, *Statistical Optics* (Wiley, New York, 1985).

24. J. A. Koch, B. J. MacGowan, L. B. Da SIlva, D. L. Matthews, J. H. Underwood, P. J. Batson, R. W. Lee, R. A. London and S. Mrowka, *Experimental and theoretical investigation of neonlike selenium x-ray laser spectral linewidths and their variation with amplification* , Phys. Rev. A50, 1877(1994)

25. D. A. Whelan, C. Keane, B. J. MacGowan, D. L. Matthews, J. E. Trebes and M. J. Eckart, , SPIE Proc. 831, 275(1987)

26. G. M. Shimkaveg, M. R. Carter, R. S. Walling, J. M. Ticehurst, J. A. Koch, S. Mrowka, J. E. Trebes, B. J. MacGowan, L. B. Da Silva, D. L. Matthews, R. A. London and R. E. Stewart, in *Lasers '91*(SPIE proceedings, Los Angeles, 1991), vol. 1551, pp. 84.

Technical Information Department • **Lawrence Livermore National Laboratory**
University of California • Livermore, California 94551